J. Physiol. (1982), **330**, *pp.* 221–242
With 6 text-figures
Printed in Great Britain

THE PASSIVE ELECTRICAL PROPERTIES OF GUINEA-PIG VENTRICULAR MUSCLE AS EXAMINED WITH A VOLTAGE-CLAMP TECHNIQUE

BY JÜRGEN DAUT

From the Physiologisches Institut der Technischen Universität München, Biedersteiner Strasse 29, 8000 München 40, Federal Republic of Germany

(*Received 30 September 1981*)

SUMMARY

1. A voltage-clamp technique was developed for stable recording of small currents in guinea-pig ventricular muscle. Small cylindrical preparations were impaled with three micro-electrodes, one for measuring the feed-back potential and two for injecting current.

2. The longitudinal potential profile resulting from current injection at one point was measured. It agreed well with the theoretical predictions for a linear cable which is sealed at both ends ('healing over'), with a length constant (λ) of 580 ± 145 μm.

3. When the clamp current was injected symmetrically into each half of the preparation via two electronic current pumps a spatially homogeneous clamp could be achieved in preparations with a diameter of $\leqslant 250$ μm and a length of $\leqslant 2\lambda$.

4. The membrane capacity and the membrane resistance of the preparations at the resting potential were measured with small voltage-clamp pulses. Assuming a specific membrane capacity (C_m) of 1 μF/cm^2 a specific membrane resistance (R_m) of $6{\cdot}7 \pm 1{\cdot}8$ kΩ cm^2 was obtained in Tyrode solution containing 3 mM-K.

5. The total surface area was calculated from the measured capacity of the preparation assuming a C_m of 1 μF/cm^2. The total cellular volume was estimated from optical measurement of the external dimensions of the preparation assuming an extracellular space of 25%. From these data the average surface/volume ratio of individual cells was calculated to be 7200 cm^2/cm^3.

6. From the measured electrical constants the specific resistance of the intracellular space (R_i) was calculated to be 200–250 Ω cm. With small constant current pulses a membrane time constant of $6{\cdot}6 \pm 1{\cdot}3$ ms was measured.

7. The influence of the extracellular potassium concentration ($[K]_o$) on R_m was studied in the range 1·5–6 mM-$[K]_o$. R_m was found to depend on $[K]_o$ less than predicted by the constant field theory.

INTRODUCTION

The reconstruction of cardiac action potentials requires a precise knowledge of (i) the passive electrical properties of the cell membrane, (ii) the time- and voltage-dependent conductance changes, (iii) the currents produced by electrogenic pumps

and ion-exchange mechanisms, and (iv) the geometry of the three-dimensional cellular network formed by cardiac tissues (McAllister, Noble & Tsien, 1975; Beeler & Reuter, 1977; DiFrancesco & Noble, 1981). However, the complexities of the electrical syncytium consisting of small cells with narrow intercellular spaces make the investigation of transmembrane currents difficult. Therefore much effort has been put into the development of voltage-clamp techniques for cardiac tissues, and the critical discussion of their capabilities and limitations has received much attention (Johnson & Liebermann, 1971; Trautwein, 1973; Attwell & Cohen, 1977; Beeler & McGuigan, 1978; Reuter, 1979).

The objective of the experiments reported here was a study of the effects of digitalis on the electrogenic sodium pump in mammalian ventricular muscle, which is published in an accompanying paper (Daut & Rüdel, 1982). In order to measure the change of the electrogenic pump current during successive application and wash-out of various concentrations of a cardiac glycoside, constant recording conditions were required for several hours. With the sucrose-gap technique the amplitude of the recorded current depends critically on the ratio of intra- to extracellular longitudinal resistance (r_i/r_o) (New & Trautwein, 1972; McGuigan & Tsien, 1974). Since both of these tend to change with time (Trautwein, 1973; Beeler & McGuigan, 1978) the variable contribution of the shunt current to the measured clamp current might make it difficult to study the concentration dependence of the effects of cardiac glycosides on the Na–K pump.

This paper describes an adaptation of the two-micro-electrode voltage-clamp technique (Deck, Kern & Trautwein, 1964; Noma & Irisawa, 1976) which can be used in mammalian ventricular muscle. Cylindrical pieces of guinea-pig ventricular muscle were impaled with three micro-electrodes, one for measuring the membrane potential and two for injecting the clamp current symmetrically into each half of the preparation. The aim was to clamp the potential of long and thin trabeculae or papillary muscles (diameter $\leqslant 250$ μm, length up to 1400 μm) in which the cut surface which had to 'heal over' after dissection was relatively small. These preparations were found to be much more viable than short ones and reproducible effects of cardiac glycosides on the membrane potential could be measured for more than 8 h.

In order to test the suitability of the technique for recording the electrogenic pump current the passive electrical properties of the preparation were measured. On the whole the results are in reasonable agreement with previous measurements. There are, however, some quantitative differences which may help to construct a more precise picture of the passive electrical properties of cardiac ventricular muscle.

Since the pioneering work of Weidmann (1952) on the passive electrical properties of cardiac Purkinje fibres only a limited amount of information about the electrical constants of mammalian ventricular muscle has accumulated. Three main approaches have been used so far. (i) Polarization of a bundle of cells by large external electrodes placed at one or both ends and mapping of the resulting intracellular and extracellular electrotonic potential (Weidmann, 1970; Sakamoto & Goto, 1970; Sakamoto, 1969; Kamiyama & Matsuda, 1966). One of the limitations of this method is that r_m (membrane resistance $\times$ unit length) and c_m (membrane capacitance per unit length) cannot be measured directly. The calculation of r_m and c_m was based on measurements of the ratio of intra- to extracellular longitudinal resistance (r_i/r_o) which may depend

on the size of the preparation and on the experimental conditions chosen. (ii) The double sucrose-gap method (McGuigan, 1974). One of the limitations of this method lies in the fact that a significant fraction of the applied current may cross the membrane in both the left-hand and right-hand sucrose regions (see McGuigan & Tsien in McGuigan, 1974). This means that it is difficult to define precisely the area of membrane which contributes to the measured resistive and capacitative currents. (iii) Injection of current through an intracellular micro-electrode (Tille, 1966; Tanaka & Sasaki, 1966; Sakamoto, 1969). The main limitation of this method – as it was applied by these authors – lies in the fact that three-dimensional spread of current must be considered in the large preparations used, which makes the analysis much more difficult.

In the technique described in this paper the methodological limitations mentioned play only a minor role. It will be shown that the spread of current in the thin preparations used (diameter $\leqslant 250$ μm) can be described by linear cable theory, and that the whole preparation can be polarized homogeneously by current injection through two micro-electrodes. In this way the membrane resistance, the membrane capacitance and the membrane time constant of the preparation can be measured directly. The length constant can be obtained from the longitudinal potential decrement recorded when injecting current through one micro-electrode, and the intracellular longitudinal resistivity can be calculated from the measured parameters. Preliminary accounts of some of the results have been published (Daut & Rüdel, 1979, 1980).

METHODS

Dissection and tissue chamber

Guinea-pigs weighing 200–250 g were killed by a blow on the head. The hearts were quickly removed and placed in a dissection chamber which was perfused with a cardioplegic solution of the following composition (mM): NaCl, 60; K_2SO_4, 60; $CaCl_2$, 4; $MnCl_2$, 1; $MgCl_2$, 0·5; Na pyruvate, 2; glucose, 20; Tris maleate buffer, 10 (pH 7·4). The solution was gassed with 100% O_2 and the temperature was held at 34 ± 2 °C.

After several contractions, which served to pump out the remaining blood, the heart relaxed. Papillary muscles or ventricular trabeculae of cylindrical shape with a diameter 250 μm or less were excised from either ventricle. In most of the guinea-pig hearts at least one suitable preparation could be found. Often long cylindrical side branches of papillary muscles in the right ventricle or fine trabecular strands near the tip of the left ventricle were used. Care was taken not to use Purkinje fibres. These are usually whiter, longer and thinner than ventricular trabeculae and they tend to give off fine side branches. Transitional forms between ventricular muscle and Purkinje fibres also exist which can be recognized by their low contractility and their electrical properties (see Results).

Immediately after dissection the preparation was sucked into a fine polythene tubing with a small syringe and transferred into the recording chamber. The recording chamber was perfused with a modified Tyrode solution of the following compostion (mM): NaCl, 117; KCl, 3; $CaCl_2$, 2; $MgSO_4$, 1; Na pyruvate, 2; $NaHCO_3$, 26·2; NaH_2PO_4, 1·67; glucose, 10. This solution was gassed with 95% O_2 and 5% CO_2 (pH 7·4). The temperature was 35–37 °C and was held constant within 0·3 °C during an individual experiment. When the potassium concentration was varied KCl was substituted for NaCl in equimolar amounts. In many experiments the dissection was also carried out in this modified Tyrode solution containing 6 mM-K. The results obtained with surviving preparations were the same; however the success rate was much higher when the dissection was performed in the cardioplegic solution described above.

The recording chamber consisted of a 1·5 mm diameter boring in a Perspex block, which was opened at the top over a distance of 8 mm for access of the micro-electrodes. It was perfused at a rate of 50–80 μl/s by means of a fine peristaltic pump built in our workshop. The open part of

the chamber contained a volume of about 10 μl solution which was kept inside by surface tension. Five millimetres behind the chamber there was a small basin from which the solution dripped out by gravity. The basin contained the temperature sensor of a digital thermometer (Newport, Santa Ana). The solution was heated by pumping it through a coil of rubber tubing placed in a water bath before the entry to the chamber. The temperature of this water bath was controlled by a separate heating and perfusion system (Haake, Berlin).

In the recording chamber the preparation was stimulated through two 0·1 mm platinum wires. Contractility was usually restored immediately; nevertheless the preparation was allowed to recover for at least 15 min at a stimulation frequency of 0·2 Hz. Subsequently it was pulled through a loop of silk thread of 50 μm diameter the ends of which were threaded through two fine borings in the side walls of the chamber and fixed to two screws. By turning these screws the loop could be tightened to separate off a section of suitable length. To facilitate impalement the preparation was then slightly stretched, supported by a piece of fine polythene tubing and fixed with insect pins at both ends. The final length of the preparation was 700–1400 μm; the diameter was 90–250 μm. This was measured optically with a dissection microscope. Three hydraulic micro-manipulators (D. Kopf, Tujunga, California) were used for impalement.

Electronic apparatus

Three micro-electrodes were used for voltage clamping (Fig. 1). One of these was connected to a conventional high input impedance ($10^{13}\Omega$) preamplifier ($\times 10$); the other two were connected to two electronic current pumps (voltage–current converters). These were similar to the one described by Dreyer & Peper (1974). The main differences were the improved capacity compensation and the use of low voltage (± 15 V) operational amplifiers. This limited the maximal current to less than 1 μA, but it had the advantage that part of the circuit could be mounted on the micro-electrode holder as a head stage. The output was 100 μA per 1 V input. The voltage-clamp mode could be switched on and off with an electronic microswitch (C in Fig. 1). When it was switched off the current pumps could be used either for measuring the membrane potential or for injecting constant current pulses. In the voltage-clamp mode the output of the inverting clamp amplifier ($\times 1000$) was connected to the inputs of one or both current pumps (switches B and C). For current injection electrodes of 10 MΩ the maximal open-loop gain of the clamp circuit was 10,000.

To achieve a spatially homogeneous clamp of the whole preparation the same current was injected into each half of the preparation at points half-way between the middle and either end (see Fig. 1). The voltage measuring electrode was usually inserted at a distance of about 1/10 of the length of the preparation from one of the current-passing electrodes. With this electrode positioning the transmembrane current measured in a preparation which behaves like a short linear cable approaches that of a perfectly space-clamped preparation (see DiFrancesco & McNaughton, 1979).

The micro-electrodes were filled with a solution of 1·5 M-KCl plus 1·5 M-K citrate and had a resistance of 5–15 MΩ. For capacity compensation they were coated with a silver paint to within 1 mm from the tip and insulated with nail polish. In part of the experiments the current-passing electrodes were coated with a similar shield which was grounded.

The grounding of the bath was provided by a clamp circuit as indicated schematically in Fig. 1. The bath potential was measured with an electrode which consisted of a polythene tubing filled with an agar bridge (1 M-NaCl, 3 % agar-agar), 1 M-NaCl solution, and a chlorided silver wire. The polythene tubing had an outer diameter of 2 mm which tapered to a fine tip (0·3 mm o.d.). It was sealed at the back with wax and held close to the preparation by a micro-manipulator. The feed-back amplifier (Burr Brown 3523) was mounted on the electrode holder. The current was fed back into the bath through a 5 MΩ resistor and a 0·1 mm platinum wire which passed alongside the preparation. With this arrangement the series resistance could be reduced to 200–300 Ω. Current was always measured both in the the bath clamp and at the input of the current pumps (Fig. 1).

Records of potentials and currents were taken on two dual beam storage oscilloscopes (Tektronix D13), a 6-channel penwriter (Linseis 2000) and a 4-channel tape recorder (Hewlett Packard 3964A). In some experiments five to twenty identical small voltage or current signals were recorded on tape and later averaged on a Nicolet 535 signal averager. The penwriter also served as a low-pass filter (-3 dB at 2 Hz). Zero back-off was used to record membrane potentials near the resting potential at high gain. The timing of command pulses was performed with a digital pulse generator (Hivotronic).

Presentation of results and statistical analysis

Fast events were photographed from the two oscilloscopes. Slow changes of current and potential were photographed from the pen recordings which were written on the back of the recording paper to eliminate the grid. Some of the traces were slightly retouched because the black and white film was less sensitive to the colours of some of the pens.

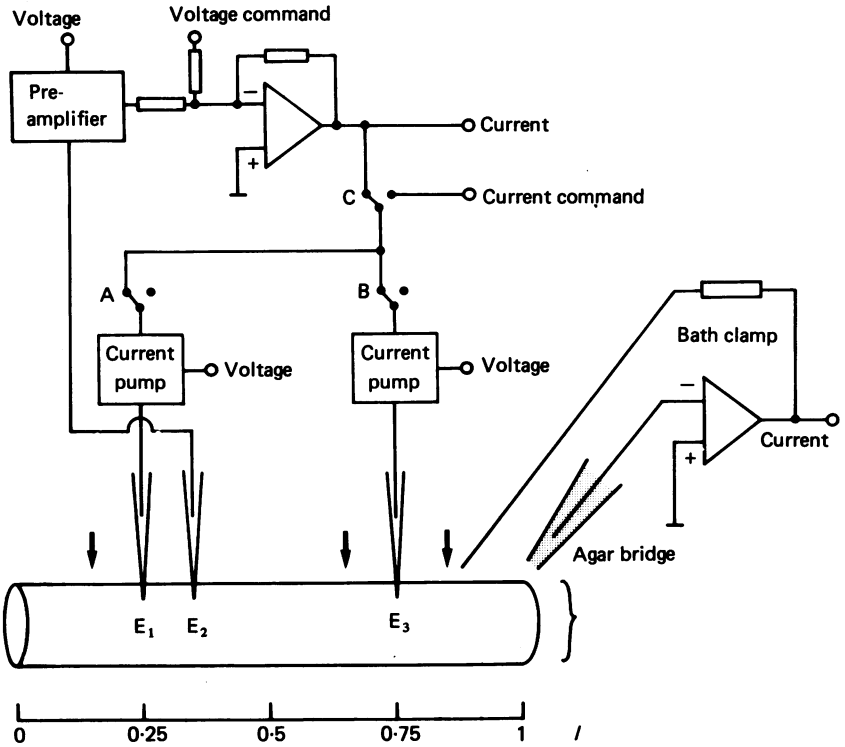

Fig. 1. Schematic diagram of the voltage-clamp circuit. Cylindrical preparations of length l were impaled with two current-passing micro-electrodes (E_1 and E_3) and a voltage-measuring electrode (E_2). Alternative positions of the voltage electrode are indicated by vertical arrows. The function of the switches A, B and C is explained in the text.

All results are reported as mean values ± standard deviation. The number of preparations (n) from which the data were obtained is given in parentheses. Some of the results were obtained with modifications of the method, but only the procedures adopted as a standard during later stages of the work have been mentioned here.

THEORY

If, near the resting potential, the preparation behaves like a linear cable which is terminated at both ends by an infinite resistance the longitudinal potential profile can be calculated from cable theory. For current injection at any point of the preparation the longitudinal potential profile is given by

$$V_x = \tfrac{1}{2}I_0 r_i \lambda . [\exp(-|x|/\lambda) - \exp((-|x|-2l)/\lambda) + \exp((-x-2d)/\lambda) + \exp((x+2d-2l)/\lambda) + \exp((-x-2l)/\lambda) + \exp((x-2l)/\lambda)] : [1-\exp(-2l/\lambda)], \quad (1)$$

where V_x is the potential at point x. x is defined as the distance (cm) from the point of current injection, being taken as negative when it is to the left and positive when it is to the right. d is the distance of the point of current injection from the left-hand end of the preparation (cm). λ is the length constant (cm). l is the length of the preparation (cm). r_i is the intracellular resistance per unit length (Ω/cm). I_0 is the injected current (A).

At the point of current injection the potential change V_0 is given by

$$V_0 = \tfrac{1}{2} I_0 r_i \lambda . [\coth (l/\lambda)] . \left[1 + \frac{\cosh ((l-2d)/\lambda)}{\cosh (l/\lambda)}\right]. \tag{2}$$

These equations were derived from the equation for an infinite RC-cable (Hodgkin & Rushton, 1946) by adding the sum of an infinite number of terms for the 'reflexions' at the sealed ends (see Jack, Noble & Tsien, 1975, chapter 4). For $d = 0$ and $x \geqslant 0$ eqns. (1) and (2) reduce to the well known equations given by Weidmann (1952; his 'case 3').

The membrane resistance (R) and the membrane capacitance (C) were measured by homogeneously polarizing the preparation with small voltage-clamp pulses near the resting potential. The total membrane surface (s) was estimated from the measured membrane capacitance of the preparation assuming a specific membrane capacitance of the preparation assuming a specific membrane capacitance (C_m) of 1 μF/cm^2. The cellular volume (v) was estimated from the total volume of the preparation measured optically assuming an extracellular space of 25 % (Page, 1962). The length constant was calculated from the longitudinal potential decrement recorded during current injection with one micro-electrode using eqn. (1).

For long cylindrical cells with infoldings of the surface membrane, the length constant can be defined as

$$\lambda = \sqrt{\left(\frac{A}{P}\right)} . \sqrt{\left(\frac{R_m}{R_i}\right)}, \tag{3}$$

where A is the cross-sectional area and P is the perimeter, R_m is the specific membrane resistance and R_i is the longitudinal resistivity (Mirolli & Talbot, 1972). Provided the length of individual cells is much larger than the radius, eqn. (3) is well approximated by

$$\lambda^2 = \frac{v}{s} . \frac{R_m}{R_i}. \tag{4}$$

Since $R = R_m/s$ eqn. (4) can be rewritten to give

$$R_i = \frac{R . v}{\lambda^2}. \tag{5}$$

Thus an estimate of R_i can be derived from the measured parameters. The extracellular resistivity has been neglected in eqns. (3)–(5) (see Results).

RESULTS

The standard procedure carried out at the beginning of each experiment is illustrated in Fig. 2. Preparations of less than 250 μm diameter were impaled with three micro-electrodes labelled E_1, E_2 and E_3 on the penwriter records shown. One of the membrane potentials was also recorded at ten times higher gain ($E_2 \times 10$, lowermost trace). After recovery from the impalements the three membrane potential measurements agreed within 2 mV. Two of the micro-electrodes (E_1 and E_3) could

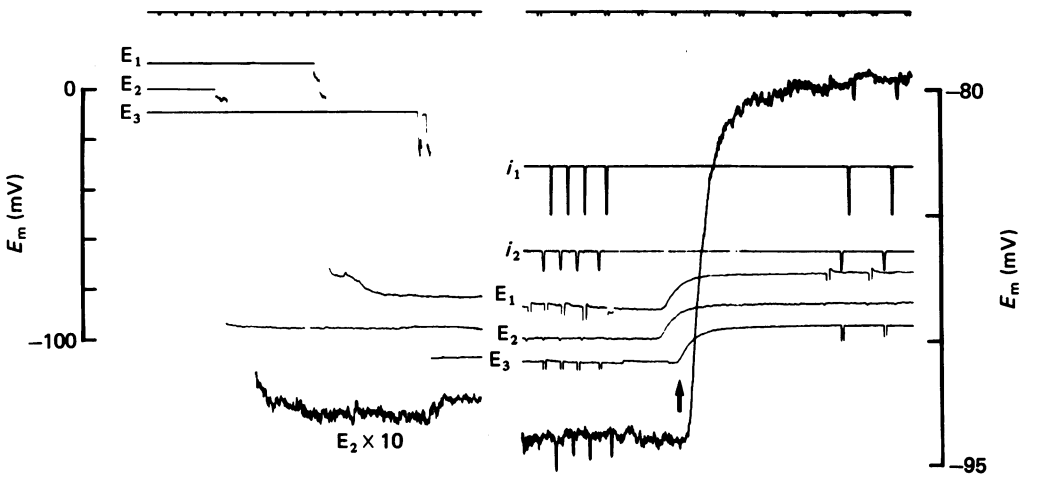

Fig. 2. Test of the recording system. Photographs of two penwriter records; the time interval between the records was 5 min. Uppermost trace: time marker, 10 s. Note that the paper speed was doubled on the right-hand record. The three impalements (E_1, E_2, E_3) are shown on the left. The left-hand ordinate denotes the potential measured at E_2; the other two membrane potential calibrations are shifted by ± 10 mV. The right-hand ordinate denotes the membrane potential measured at $10 \times$ higher gain ($E_2 \times 10$). The amplitude of the current pulses recorded both at the input of the current pumps (i_1) and in the bath clamp (i_2) was 40 nA. The potential traces of the two current-passing electrodes (E_1 and E_3) went off scale during the current pulses. The penwriter traces are slightly shifted on the time axis. Some of the traces were retouched (see Methods). The arrow indicates the change from 3 to 6 mM external K.

be used for injecting current via electronic current pumps. The current command applied at the input of the current pumps is labelled i_1, the current recorded in the bath clamp is labelled i_2. When negative current pulses of 40 nA amplitude were applied through two micro-electrodes (E_1 and E_3) a hyperpolarization of about 1 mV was recorded on the low and high gain records of the third electrode (E_2). Note that the six traces of the penwriter are slightly shifted on the time axis.

At the vertical arrow the K concentration of the modified Tyrode solution was stepped from 3 to 6 mM and a depolarization of about 14 mV was recorded by all three micro-electrodes. Modified solution containing 3 mM-K was used as a standard because a high membrane resistance was considered desirable for voltage clamping. The average resting potential was -94 ± 2 mV ($n = 60$). The membrane potentials

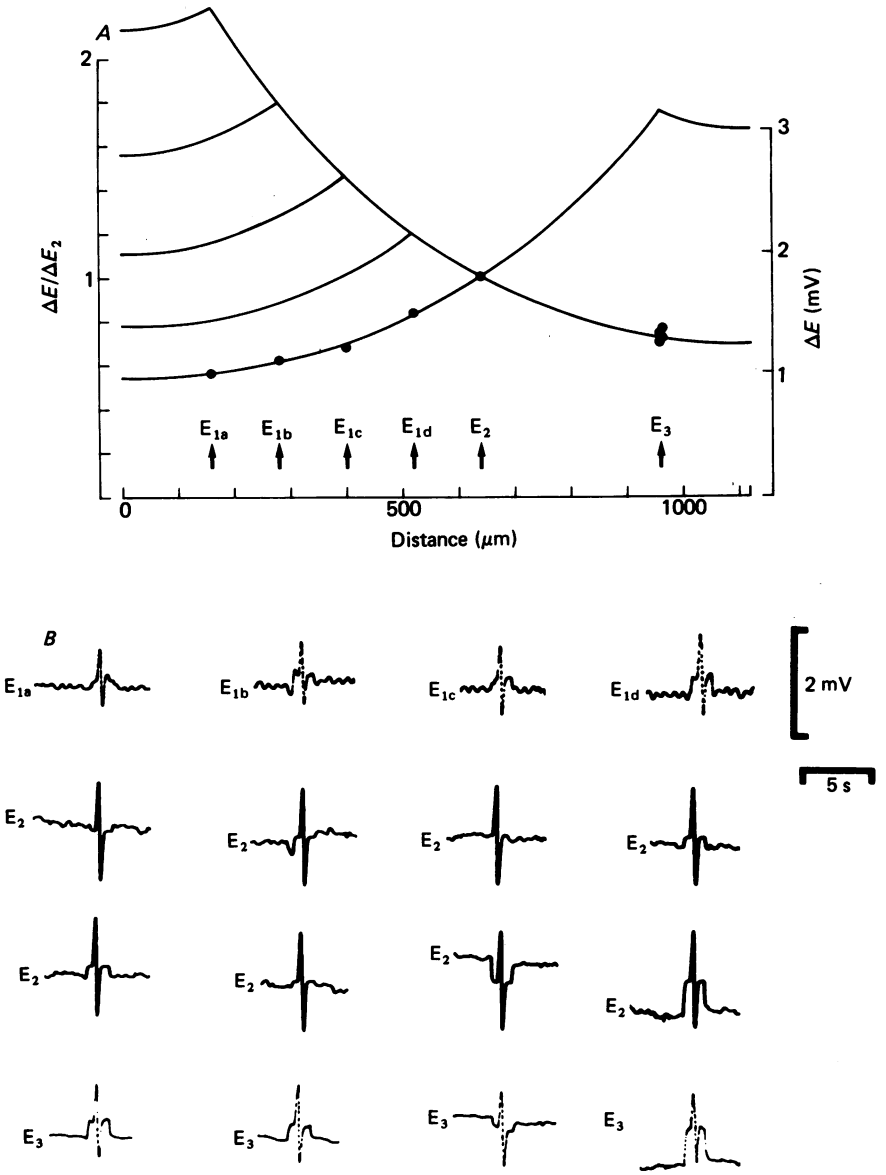

Fig. 3. The longitudinal potential profile in a preparation of 1120 μm length and 130 μm diameter. *A*, the peak-to-peak amplitude of the voltage deflexions (right-hand ordinate) measured at six different points (arrows) along the axis of the preparation (abscissa). Ramp-shaped voltage commands ($\pm$0·9 mV) were imposed on the voltage feed-back electrode (E_2). Only one of the current-passing electrodes (E_1 or E_3) was included in the voltage-clamp loop, whereas the other one was used to record the attenuation of the voltage deflexion imposed on E_2 (see Fig. 1). The left-hand current electrode was moved successively from E_{1a} to E_{1d}. The normalized amplitude of the potential deflexions ($E_2 = 1$) can be read from the left-hand ordinate. The continuous lines represent the longitudinal potential profile calculated from cable theory for current injection at

were also continuously recorded on two oscilloscopes and it was checked that ventricular action potentials of the same configuration were recorded by the three micro-electrodes. A typical action potential is shown in Fig. 5*B*. In some experiments a small hyperpolarization and a prolongation of the action potential were observed after several hours, otherwise the preparations appeared to be in a very stable condition during the entire experiment (8–12 h).

The length constant and the longitudinal potential profile

The first objective was to see if the spread of current in the preparation could be described by linear cable theory. To investigate the longitudinal potential decrement along the preparation only one of the current injection electrodes (E_1 or E_3) was included in the voltage-clamp loop while the other one was used for measuring the membrane potential at high gain. In this way a voltage deflexion imposed on the feed-back electrode (E_2) could be compared with the voltage signal at various other points along the preparation. Ramp-shaped voltage commands were preferred to steps for practical reasons: the signals had to be slow enough to be recorded faithfully by the penwriter and at the same time it was tried to minimize the total clamp current in order to avoid extracellular K accumulation or depletion (see Discussion). A typical experiment is shown in Fig. 3. The positions of the electrodes E_1, E_2 and E_3 on the longitudinal axis of a preparation of 1120 μm length are marked by arrows (Fig. 3*A*). It can be seen that the voltage feed-back electrode E_2 was always kept in the same place, whereas electrode E_1 was successively inserted at four different points E_{1a}–E_{1d}.

The potentials recorded when electrode E_1 was in position E_{1a} are shown in the first column of Fig. 3*B*. The upper two records show that during a ramp-shaped voltage command the potential recorded at E_1 was only about half as large as the voltage recorded at the feed-back electrode, E_2. The peak to peak amplitude of the two voltage deflexions are plotted at the corresponding electrode positions in Fig. 3*A*. Subsequently the function of electrodes E_1 and E_3 was exchanged: E_1 was used for injecting the clamp current and E_3 was used as a second potential measuring electrode. The lower two records of the first column of Fig. 3*B* show the potential changes recorded under these conditions. It can be seen that the peak-to-peak amplitude of the ramp is reduced by a factor of 0·7 at E_3 as compared to E_2. This is also plotted in Fig. 3*A*.

After that the left-hand electrode was withdrawn and successively inserted at three other points E_{1b}, E_{1c} and E_{1d}. The same sequence of records as described above was obtained at each electrode position. Each column of Fig. 3*B* represents one position of electrode E_1; the upper two traces in each column were obtained during current

---

positions E_{1a}–E_{1d} and E_3, respectively, using a value of 520 μm for λ. *B*, the penwriter records of the data plotted in *A*. Each column represents one of the positions of the left-hand electrode (E_1). The upper two records of each column show the potential deflexions recorded at E_1 and E_2 when the clamp current was injected at E_3; the lower two records show the potentials recorded at E_2 and E_3 when the clamp current was injected at E_1. The voltage clamp was switched on for 2 s during each run. The holding potential (on which the ramp-shaped voltage command was superimposed) was −93 mV throughout. It can be seen that there were small (< 1 mV) changes in resting potential between different records.

injection through E_3, the lower two during current injection through E_1. The voltage command was a ramp of 1·8 mV peak-to-peak amplitude throughout the experiment. Therefore the plot of the voltage deflexions recorded at various points of the preparation (Fig. 3*A*) represents the longitudinal potential profile during current injection at one point.

The continuous lines in Fig. 3*A* were obtained by calculating the longitudinal potential profile in a linear cable of 1120 μm length for current injection at various points (E_3, E_{1a}–E_{1d}) using eqn. (1). The only free variable was the length constant, λ. By trial and error a value of 520 μm for λ was found to fit all of the data points. Thus it appears that near the resting potential the preparation did indeed behave like a linear cable which is terminated at both ends by an open circuit. Such a detailed analysis of the longitudinal potential profile was carried out in four experiments with very similar results.

A spatially homogeneous clamp of the whole preparation was achieved by injecting current through two micro-electrodes. In most of these experiments a simplified procedure for determining λ was used which is illustrated in Fig. 4. The preparation was impaled with three micro-electrodes at the positions marked by arrows (Fig. 4*A*). The potential decrement between E_2 and E_1 (left in Fig. 4*B*) and between E_2 and E_3 (middle) was determined by switching from one current injection electrode to the other as explained above. The potential deflexions measured at E_1, E_2 and E_3 are plotted in Fig. 4*A* (filled circles). The potential profiles calculated for current injection at E_1 and at E_3 could both be fitted to the experimental data with a length constant of 700 μm (continuous lines).

Subsequently both current electrodes (E_1 and E_3) wer included in the voltage-clamp loop and the same ramp-shaped voltage command was applied (right in Fig. 4*B*). The potential profile expected for current injection at both E_1 and E_3, which was calculated from cable theory using the length constant of 700 μm determined before, is shown in Fig. 4*A* (dashed line). It can be seen that in this case the preparation is clamped homogeneously with deviations of less than 10 % from the voltage ramp imposed on E_2.

If the calculated curves are a correct description of the longitudinal potential distribution the currents measured during the three voltage-clamp runs should be proportional to the total current defined by the area under the curves. The relative magnitude of the currents calculated from the area under the corresponding potential profile were 1·27, 0·87, and 1·02, the current for a perfect space clamp being taken as 1. This is in good agreement with the currents recorded at the input of the current pumps (i_1) and in the bath clamp (i_2) which are shown in the lower traces of Fig. 4*B*. The peak-to-peak amplitude of the currents recorded during the three voltage-clamp runs was 147, 96 and 115 nA, respectively (relative amplitudes: 1·28; 0·87; 1).

From these results it appears that the potential profile obtained during current injection through two micro-electrodes does indeed correspond to the theoretical curve calculated from cable theory (dotted line in Fig. 4*A*). Moreover the currents measured with the three-micro-electrode clamp seem to correspond quite well (within 2 % in the example shown) to those of a perfectly space-clamped preparation.

As a control of this interpretation the absolute value of i_m (membrane current per unit length) was calculated in two different ways. Firstly r_m (membrane

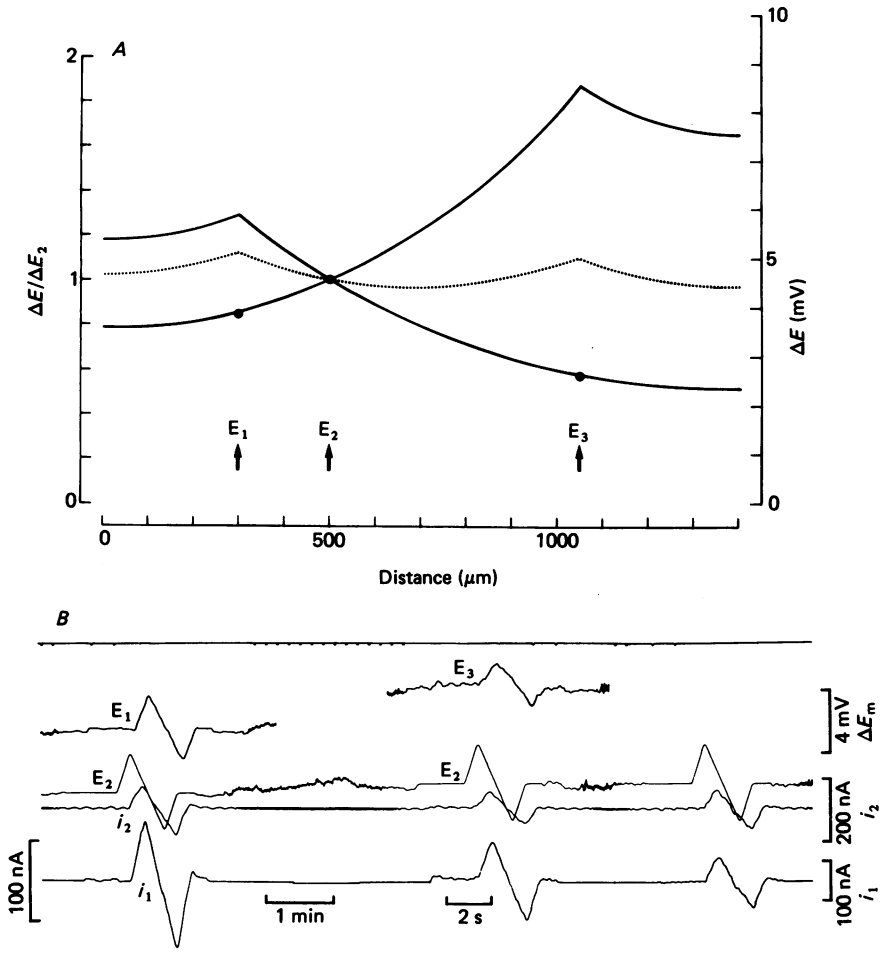

Fig. 4. The longitudinal potential profile in a preparation of 1400 μm length and 160 μm diameter, and the corresponding clamp currents. *A*, plot of the voltage deflexions measured at E_1, E_2 and E_3. Co-ordinates as in Fig. 3*A*. The continuous lines represent the longitudinal potential profile calculated from eqn. (1) for current injection through either E_1 or E_3, using a value of 700 μm for λ. The dotted line shows the longitudinal potential profile calculated with the same value of λ for current injection through both electrodes (E_1 and E_3). *B*, penwriter records of the data plotted in *A*. Two paper speeds were used, see calibration bars at the bottom and the time marker (top trace, 10 s intervals are marked by double pulses). The clamp was switched on three times for 6 s; the same ramp-shaped voltage command was given each time. On the left (current injection at E_3) the potentials at E_2 and E_1 were recorded. During the second ramp (current injection at E_1) the potential decrement between E_2 and E_3 was recorded (middle). Subsequently both current injection electrodes were included in the voltage-clamp loop and another ramp-shaped voltage command was given (right). The corresponding currents recorded in the bath clamp are labelled i_2, and the currents recorded at the input of one or both current pumps (see Fig. 1) are labelled i_1. Note that the calibration of i_1 changes by a factor of 2 when current is injected with both current pumps (right-hand calibration bar).

resistance × unit length) was calculated from the right-hand record of Fig. 4*B* (assuming uniform polarization) and i_m at E_1 ($= \Delta E_1/r_m$) was calculated from the left-hand record of Fig. 4*B*. Secondly i_m at E_1 was estimated from the potential decrement between E_2 and E_1 using eqn. (2) of Kass, Siegelbaum & Tsien (1979). The value of r_i (resistance × unit length) inserted in this equation was calculated assuming a longitudinal resistivity of 225 Ω cm (see below) and an extracellular space of 25 %. The values of i_m at E_1 obtained by the two methods were $6{\cdot}9 \times 10^{-7}$ and $6{\cdot}2 \times 10^{-7}$ A/cm, respectively. The reasonable agreement of the two estimates of i_m corroborates the hypothesis that the spread of current in the preparation can be described by one-dimensional cable theory.

In some experiments λ was determined by applying constant current pulses (instead of voltage-clamp ramps) successively through either current pump. The average length constant measured in twenty-five preparations was 580 ± 140 μm.

Membrane capacitance, surface/volume ratio and membrane resistance

To determine the membrane resistance (R) and the membrane capacitance (C) of the whole preparation spatially uniform voltage-clamp pulses were applied. Preparations were considered acceptable for such experiments only if they were not longer than two length constants. C was measured with rapid voltage-clamp ramps. Fig. 5*A* shows that every change in dV/dt was associated with a jump in the current record (see Dudel, Peper, Rüdel & Trautwein, 1966) from which the membrane capacitance can be calculated. The capacitative transient following a voltage step was not used for determining C because its peak was usually cut off as a result of the limited current passing capacity of the current pumps.

It is difficult to calculate the specific membrane capacitance (C_m) from these data because the precise surface/volume ratio of guinea-pig ventricular muscle is not known. On the other hand a specific membrane capacitance of 1 μF/cm² is a widely accepted constant of biological membranes (Cole, 1968). Therefore the measured capacitance of the preparation was used to obtain an estimate of the total membrane surface (s) of the preparation assuming C_m to be 1 μF/cm². The cellular volume (v) of the preparation was deduced from the dimensions of the cylindrical preparations measured optically on the assumption of an extracellular space of 25 % (Page, 1962). From the estimates of s and v the surface/volume ratio of individual preparations was calculated. The average surface/volume ratio obtained in this way was 7200 ± 2600 cm²/cm³ ($n = 8$).

The specific membrane resistance (R_m) was usually calculated from the membrane resistance measured at the resting potential and the estimate of the surface area described above. In preparations in which C was not measured the surface area was estimated by multiplying v with the *average* surface/volume ratio given above. The average specific membrane resistance was 6730 ± 1180 Ωcm² ($n = 20$).

The intracellular resistivity and the membrane time constant

The specific resistance of the sarcoplasm (R_i) can be calculated from R, v and λ. Using eqn. (5) an average value of 260 Ω cm was obtained for R_i, which is about 5 times the resistivity of normal Tyrode solution. In eqn. (5) the resistivity of the extracellular space was neglected. If the ratio between intracellular and extracellular

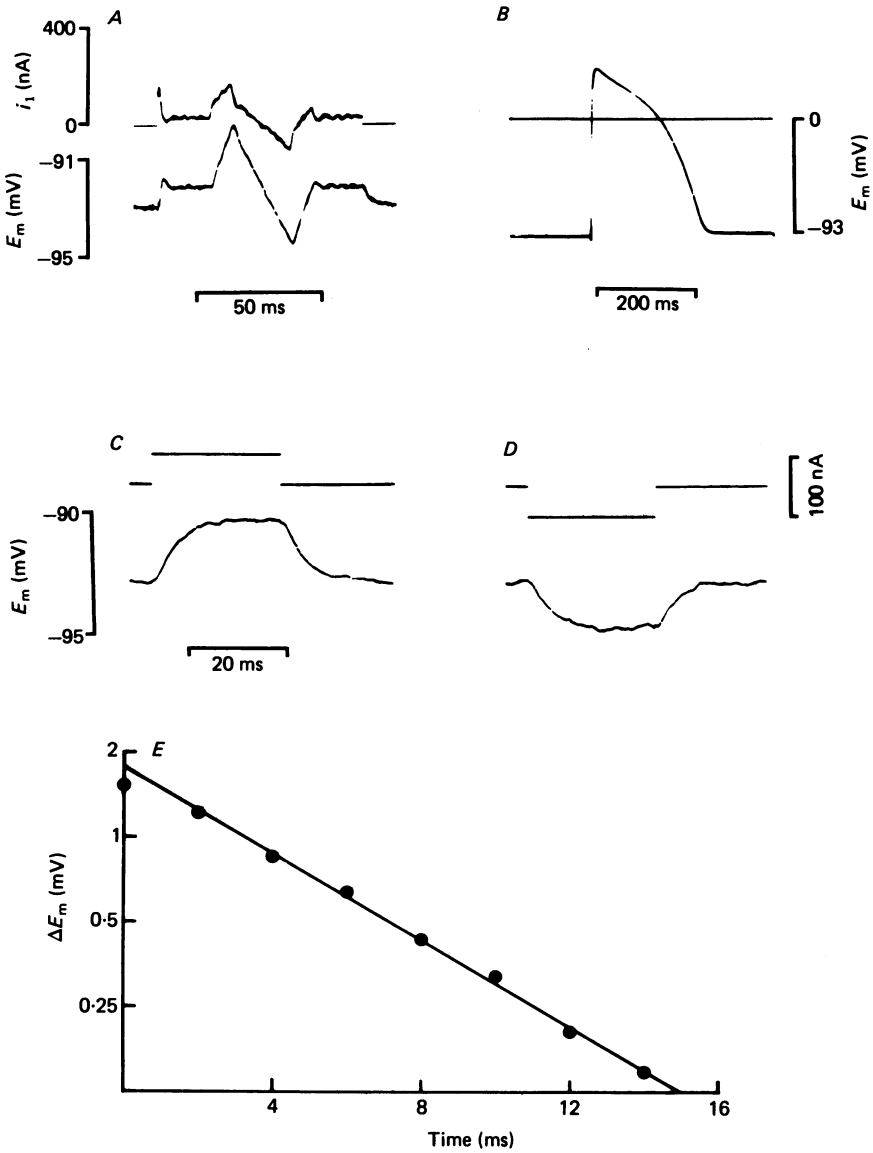

Fig. 5. Oscilloscope records of fast events. *A*, measurement of membrane capacitance. Upper trace: clamp current recorded at the current pump; lower trace: membrane potential. The clamp was switched on and off electronically. *B*, action potential in 3 mM-K Tyrode; the straight line indicates zero potential. *C*, constant outward current pulse (upper trace) and the corresponding membrane potential change (lower trace). *D*, inward (hyperpolarizing) current pulse. Records *A–D* from the same preparation (length 950 μm, diameter 150 μm). *E*, semilogarithmic plot of the decay of ΔE_m after a rectangular current pulse. Average of six traces recorded at intervals of 100 ms. The straight line in this graph was fitted to the data by linear regression of all points except the first one.

longitudinal resistance is taken to be 3 : 1 (Weidmann, 1970; Clerc, 1976) a value of 195 Ω cm is obtained for R_i. However, the preparations used by Weidmann and Clerc were about four times larger in diameter, so one might expect a smaller contribution of the resistivity of the extracellular space in the experiments reported here. Therefore the actual value of R_i in guinea-pig ventricular muscle is probably between 200 and 250 Ω cm.

The membrane time constant (τ) was determined by injecting a constant current pulse through both current pumps. As can be seen from Fig. 5*C* and *D* the resulting voltage deflexion had a brief initial sigmoid phase and was roughly exponential at later times. Fig. 5*E* shows the results of a typical experiment in which the voltage change produced by six identical current pulses was averaged on a Nicolet 535 signal averager and plotted on a semilogarithmic scale. The sigmoid phase usually lasted 2–4 ms; at later times the data were well approximated by a straight line. The average time constant obtained in this way was $6{\cdot}6 \pm 1{\cdot}3$ ms ($n = 12$).

This estimate of τ is liable to some uncertainties since the time course of the voltage change after a long lasting current pulse depends both on the electrotonic length of the cable and on the site of measurement. In a short cable of 1 λ length the time course of the voltage change is expected to be slightly faster than exp $(-t/\tau)$ if the recording electrode is very close to the site of current injection (see Jack *et al.* 1975, fig. 4.10). On the other hand it was found in several experiments that with increasing distance from the point of current injection the duration of the sigmoid phase increased and the speed of the recorded voltage change decreased, as one would expect from linear cable theory (Hodgkin & Rushton, 1946).

Since the distance of the potential-recording electrode from the point of current injection was usually 0·15–0·20 λ (see Methods) it is likely that the measurement of the final potential decay yielded a reasonable estimate of τ (see also Fig. 4·9 of Jack *et al.* 1975). This view is corroborated by the fact that the time constant measured with constant current pulses (6·6 ms) agrees well with the product of $R_m \times C_m$ (6·7 ms) measured in voltage-clamp experiments. Note that ($R_m \times C_m$) is independent of the surface/volume ratio.

In individual experiments τ and ($R_m \times C_m$) agreed much better than one would expect from the scatter in the measurements of both τ and R_m. This suggests that the scatter in these measurements is only partly due to limitations of the method. It may be the result of a variability of specific membrane resistance in preparations taken from different regions of either ventricle. Furthermore, in several preparations a slightly faster early repolarization phase of the action potential, increased values of R_m (> 10,000 Ω cm²), and τ (> 10 ms), and a lower surface/volume ratio were found. Such preparations were not included in the present study because they are regarded as transitional forms between ventricular muscle and Purkinje fibres.

The effects of external potassium on membrane conductance

The membrane conductance (g_m) of cardiac ventricular muscle increases with increasing external potassium (McDonald & Trautwein, 1978; Boyett, Coray & McGuigan, 1980) and with hyperpolarization (Beeler & Reuter, 1970; Trautwein & McDonald, 1978). A corresponding difference in the potential displacement produced by hyperpolarizing and depolarizing current pulses ('anomalous rectification') can

also be seen in Fig. 5*C* and *D*. The potassium conductance (g_K) of membranes showing anomalous rectification is usually described as depending on two factors, the K driving force ($E_m - E_K$) and external K concentration (Katz, 1949; Noble, 1965). However, it is not clear whether the K conductance of cardiac preparations at the resting potential changes with external K in the way predicted by the constant field

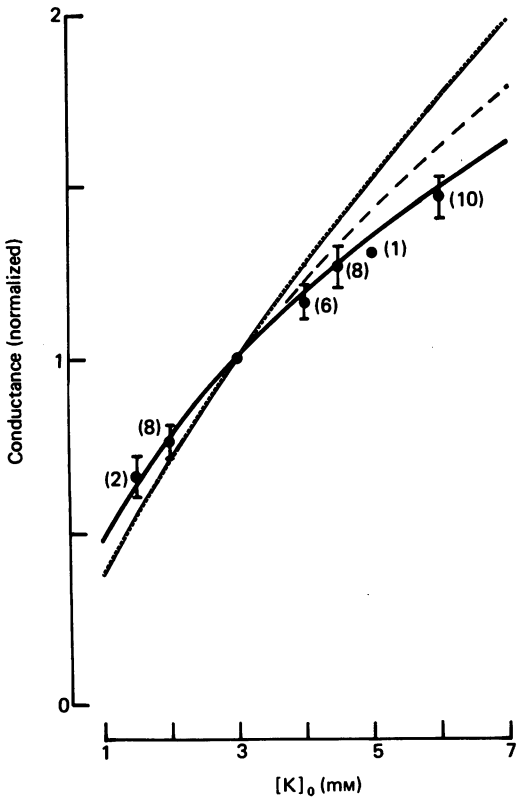

Fig. 6. The relative membrane conductance measured at various values of $[K]_o$ (1·5–6 mM) in eighteen preparations. The data were normalized, g_m in 3 mM-K being taken as 1. The points are means (±S.D., vertical bars), the number of preparations tested at each $[K]_o$ is given in parentheses. The dotted line represents the normalized g_K calculated from the Goldman equation. The interrupted line represents the resulting change in g_m expected in the presence of a constant 'background conductance' (20% of g_K at 3 mM-K). The continuous line represents the normalized g_m calculated from eqn. (6). All lines were computed using an empirical equation which describes the measured resting potential as a function of $[K]_o$.

theory (Hodgkin & Katz, 1949). In some cardiac preparations the increase of g_K with increasing $[K]_o$ could be described by the Goldman equation (Hall, Hutter & Noble, 1963; Horres, Aiton & Lieberman, 1979). In various other inward rectifying K channels, including frog ventricular muscle, the function relating g_K to $[K]_o$ was found to be less steep than one would expect if the K permeability remained constant (Almers, 1971; Ohmori, 1978; Cleemann & Morad, 1979*b*, eqn. (2.16)).

In order to examine this question the resting membrane conductance was

measured at various external K concentrations. This was done by injecting constant current pulses (see Fig. 2) or by applying small voltage ramps as in Fig. 4. In thirty-five experiments g_m measured at various $[K]_o$ was compared with the g_m measured at an external K concentration of 3 mM. In Fig. 6 the relative membrane conductance is plotted against $[K]_o$ (●). These experimental data were compared to the relation between $[K]_o$ and g_K calculated from the Goldman equation (dotted line) using the average resting potentials measured at various $[K]_o$. The intracellular K concentration was assumed to be 150 mM.

The reason for making this comparison was the notion that the resting membrane conductance is mainly determined by g_K. Since the resting potential is much closer to E_K than to E_{Na} the resting Na conductance (g_{Na}) is probably less than 10% of g_K at an external K concentration of 3 mM. The Cl conductance (g_{Cl}) may also be less than 10% of g_K. In Purkinje fibres Fozzard & Lee (1976) estimated an upper limit of g_{Cl}/g_K of 0·17. However, in their calculation of g_{Cl}/g_K neither the effects of Cl ions on the potassium conductance (Carmeliet & Verdonck, 1977) nor the effects of carrier-mediated anion-exchange mechanisms (Vaughan-Jones, 1979*a*, *b*) were taken into account. Therefore, as the latter authors pointed out, g_{Cl} may be much smaller than assumed previously. The contribution of the resting Ca conductance to g_m can probably be neglected (see Daut & Rüdel, 1982).

These considerations suggest that the contribution of conductances other than g_K to the resting membrane conductance are probably less than 20% in 3 mM-K, which implies that the increase of g_m following an increase of $[K]_o$ should be at least 80% of the increase of g_K. This is indicated by the interrupted line in Fig. 6. It can be seen that a K conductance obeying the Goldman equation cannot explain the results obtained at $[K]_o > 3$ mM when a constant 'background conductance' ($g_{Na}+g_{Cl}+g_{Ca}$) is assumed to contribute 20% to g_m at 3 mM-K. A 'background conductance' of 40% (which is rather unlikely) would have to be invoked to explain the measured dependence of g_m on $[K]_o$ on the basis of the constant field theory.

Noble (1965) has proposed that g_K may depend both on $[K]_o$ as described by the Goldman equation and on (E_m-E_k). Including such an effect of the potassium driving force on g_K in the calculation would make the discrepancy between the theoretical curve and the measured results even larger.

The continuous line was calculated from

$$g_K = \left[1+\exp\frac{z'F}{RT}(E_m-E_K-E_h)\right]^{-1}\cdot([K]_o)^{\frac{1}{2}}. \quad (6)$$

This empirical equation was used by Hagiwara & Takahashi (1974) to describe the inward rectifier channel of a starfish egg cell (see also Hille & Schwarz, 1978). F, R and T are the usual thermodynamic quantities. z' is the effective valence of a gating particle or of a blocking ion, which was taken as 1. E_h denotes the displacement from E_K at which g_K is reduced to one half; a value of 40 mV was used to calculate the curve shown. It can be seen from Fig. 6 that eqn. (6) describes the correlation between $[K]_o$ and g_m measured in guinea pig ventricular muscle reasonably well. No correction for the background conductance has been introduced in this case, but any background conductance from 0–20% can be easily accounted for by changing E_h. The main point is that eqn. (6) gives a convenient empirical description of the measured results and that, for $[K]_o > 3$ mM, g_m was roughly proportional to the square root of $[K]_o$.

To facilitate comparison with other work an estimate of the specific membrane resistance at various extracellular K concentrations was obtained. This was done by multiplying the average relative membrane resistance ($= 1/g_m$ from Fig. 6) at six different K concentrations by the specific membrane resistance determined in 3 mM-K (6·73 kΩ cm²). These values of R_m at various values of $[K]_o$ are listed in Table 1.

TABLE 1. Specific membrane resistance (R_m) at various values of $[K]_o$

$[K]_o$ (mM)	R_m (kΩ cm²)
1·5	9·9
2	8·9
3	6·7
4	5·8
4·5	5·3
5	5·2
6	4·6

DISCUSSION

Some comments on the technique

Spatial uniformity of the clamp. The longitudinal potential profile of cylindrical preparations of guinea-pig ventricular muscle (diameter 90–250 μm) was found to agree with the theoretical predictions for a linear cable with sealed ends. This implies that the radial potential decrement should be negligible. To test this, the position of one of the micro-electrodes was shifted transversely in several experiments. No systematic difference in the potential deflexions measured during injection of constant current pulses was found when the recording electrode was moved from one side of the preparation to the other. A theoretical estimate of the radial length constant on the basis of anatomical data was obtained from eqn. (11*a*) of Colatski & Tsien (1979). Assuming a width of the extracellular clefts of 1 μm (Sommer & Johnson, 1968; Johnson & Lieberman, 1971) and a resistivity of the extracellular space of 51 Ω cm (Weidmann, 1952) a radial length constant of 812 μm was calculated. Thus the radial length constant was probably several times larger than the diameter of the preparations.

These findings suggest that in the present experiments unidimensional cable analysis is sufficient to describe the spatial potential distribution, and that a uniform clamp of short preparation ($l \leqslant 2\lambda$) could be achieved by using two current-injection electrodes. In contrast, 'point polarization' of the much larger cardiac preparations used by other authors was found to be better described by two-or three-dimensional cable models (Woodbury & Crill, 1961; Tanaka & Sasaki, 1966; Sakamoto, 1969; Chapman & Fry, 1978).

Extracellular K accumulation. Extracellular K accumulation and depletion markedly influences the voltage-clamp currents recorded in sheep Purkinje fibres (Cohen, Daut & Noble, 1976*a*, *b*; Baumgarten & Isenberg, 1977). Even in cardiac ventricular muscle, although the extracellular space is nearly 100 times larger, the analysis of slow membrane conductance changes is limited by changes in extracellular K (McDonald & Trautwein, 1978; Cleeman & Morad, 1979*a*; Boyett *et al.* 1980). To obtain an estimate of the amount of K accumulation involved in the present

experiments the transient 'after-potentials' (see Cleemann & Morad, 1979*a*) following a voltage-clamp step were analysed. Within the range studied (±10 mV) the amplitude of these after-potentials was positively correlated with the amplitude and duration of the voltage step and with the radius of the preparation. With voltage steps of up to 5 mV amplitude and 0·5–1 s duration after-potentials of 100–200 μV were observed (see Daut & Rüdel, 1982), which corresponds to a K accumulation of 50 μM. With clamp currents comparable to those used to measure λ and R_m (< 0·5 μA/cm^2) after-potentials were hardly detectable at all. Therefore it is considered unlikely that accumulation artifacts distorted the results reported here.

The metabolic state of the preparation. The electrical properties of the preparations used remained constant for many hours. In preliminary experiments it was found that the electrical properties of larger preparations (diameter > 400 μm) tended to change slowly. This may be due to differences between superficial cells and cells in the centre of the preparation. A small radius seems to be advantageous for maintaining the original metabolic state of the preparation. Another factor which appears to be crucial in this respect is the ratio between the intact surface and the cut surface which has to heal over after dissection. The use of two current injection electrodes improves this ratio because it increases the length of the preparation that can be clamped homogeneously by a factor of 2. The use of the cardioplegic solution described in the Methods section may also be of value for obtaining viable preparations. It increased the success rate of the dissection considerably.

Conclusion. The small radius of the preparations used offers a number of considerable advantages for electrophysiological studies. The technique described appears suitable for measuring the cable properties of guinea-pig ventricular muscle and small current changes near the resting potential (Daut & Rüdel, 1982).

The electrical constants of mammalian ventricular muscle

The surface/volume ratio of 7200 cm^2/cm^3, calculated on the assumption of a specific membrane capacitance of 1 μF/cm^2, appears plausible. The diameter of individual cells was about 10 μm (F. Hammersen, personal communication), giving a surface/volume ratio of 4200 cm^2/cm^3 if the cell is assumed to be a smooth cylinder of 100 μm length. This leaves a factor of 1·8 for the enlargement of the surface by folding of the cell membrane and the T-system. On the basis of morphometric measurements, Page (1978) estimated the surface/volume ratio of rabbit ventricular muscle to be 5600 cm^2/cm^3. Taking into account the somewhat larger diameter of these cells this allows for a factor of 1·6–2 for the enlargement of surface area as compared to a smooth cylinder. Thus the present results are consistent with the anatomical data available, and the assumption of a specific membrane capacitance of 1 μF/cm^2 may be justified.

The specific membrane resistance was found to be 6·7 kΩ cm^2 in Tyrode solution containing 3 mM-K. Using eqn. (6) a specific resistance of 4·8 kΩ cm^2 was interpolated for 5·4 mM-K. This is in reasonable agreement with the value of 5·3 kΩ cm^2 given by McGuigan (1974) but contrasts with the value of 9·1 kΩ cm^2 given by Weidmann (1970). Both authors used sheep and cow ventricular muscle and a solution containing 5·4 mM-K. The reason for this discrepancy between Weidmann's (1970) results and mine is not entirely clear. It may be related partly to the uncertainty of the morphological data used and partly to the limitations of the methods. In view of the

similarity of the time constant measured in 5·4 mM-K ($\simeq$ 4·5 ms) it is considered less likely that the discrepancy is mainly due to species differences. It should be noted that in Weidmann's (1970) results ($R_m \times C_m$) was 1·68 . τ_m, which may suggest that either R_m or C_m was over-estimated. On the other hand his value of R_m was derived on the assumption of a surface/volume ratio of 2700 cm^2/cm^3. Taking a higher surface/volume ratio as suggested by morphometric measurements would make the discrepancy between his measurements and the present results even larger.

The length constant determined in 3 mM-K Tyrode solution was 580 μm. In three experiments λ was determined in both 3 and 6 mM-K. From these results it appears that λ is proportional to $R_m^{\frac{1}{2}}$, as one would expect from cable theory. Therefore the length constant in 5·4 mM-K was estimated to be about 500 μm. Again this is lower than the value of λ given by Weidmann (1970) (880 μm) and others (Sakamoto, 1969; Sakamoto & Goto, 1970), but it is comparable with McGuigan's (1974) results (650 μm).

The specific resistance of the intracellular space (R_i) was estimated to be 200–250 Ω cm. This is in agreement with the value of R_i determined with ^{42}K diffusion experiments (240 Ω cm; Weidmann, 1966), but it is somewhat lower than the value calculated by Weidmann (1970) on the basis of his electrophysiological experiments (470 Ω cm). It may also be compared with the values given for ungulate Purkinje fibres (181 Ω cm; Weidmann, 1970) and for rabbit Purkinje fibres (350–530 Ω cm; Colatsky & Tsien, 1979). The value of the time constant determined in the present experiments (6·6 ms; 3 mM-K) is in good agreement with Weidmann's (1970) results (4·4 ms; 5·4 mM-K) if the effects of extracellular K are taken into account.

The final conclusion is that on the whole the cable constants of cardiac ventricular muscle measured with the three-micro-electrode voltage-clamp technique are comparable to those obtained with other methods. However, the values of the specific membrane resistance and of the length constant of guinea-pig ventricular muscle reported here are somewhat lower than those measured previously in mammalian ventricular muscle.

The effects of external K on membrane conductance

The resting membrane conductance (g_m) was found to increase approximately with the square root of the external K concentration in the range 3–6 mM-K (Fig. 6). This result is at variance with the measurements of the $[K]_o$-dependence of the efflux of radioactively labelled K ions (Carmeliet, 1961; Goerke & Page, 1965; Haas, Glitsch & Kern, 1977). Working with different cardiac preparations these authors found that the dependence of potassium efflux on external K agreed with the predictions of the Goldman equation. The reason for this discrepancy is not clear. However, it has been pointed out recently that transmembrane K flux in low $[K]_o$ may be seriously underestimated as a result of re-uptake of labelled K and diffusional limitations in the extracellular clefts of cardiac preparations (Horres & Lieberman, 1977; Horres *et al.* 1979). Interestingly, Carmeliet & Verdonck (1977) recently also found that K efflux from cardiac ventricular muscle increased with $[K]_o$ less than predicted from constant field theory.

On the other hand my results are in good agreement with previous electrophysiological measurements. In cardiac Purkinje fibres Dudel, Peper, Rüdel & Trautwein

(1967) found that g_K at the K equilibrium potential was doubled when $[K]_o$ was increased from 2·7 to 10·8 mM (p. 312). The K conductance of various other inward rectifying membranes has also been shown to increase approximately with $[K]_o^{\frac{1}{2}}$ (Almers, 1971; Hagiwara & Takahashi, 1974; Ohmori, 1978; Leech & Stanfield, 1981). A variety of physical models which allow for a dependence of g_K on $[K]_o^{\frac{1}{2}}$ has been constructed recently (Armstrong, 1975; Ciani, Krasne, Miyazaki & Hagiwara, 1978; Hille & Schwarz, 1978; Cleeman & Morad, 1979*b*). Although the data reported here cannot be used to discriminate between these models, it may be worth noting that they would be compatible with a monovalent blocking ion determining the conductance of a K-selective pore ($z' = 1$ in eqn. (10); see Hille & Schwarz, 1978; Hagiwara & Yoshii, 1979). In view of the similarity of the present results with those obtained in other inward rectifying membranes it is tempting to speculate that there may be a common mechanism which controls the conductance of such K-selective channels. It would be interesting to see whether a re-investigation of the $[K]_o$ dependence of K efflux in very small cardiac preparations confirms this hypothesis.

I wish to thank Mrs Ch. Dengler for unfailing technical assistance, Mrs L. Bauer and Mrs M. Griessl for efficient secretarial help, Mr L. Müller for manufacturing the recording chamber and Mr W. Zeitz for skilful electronic engineering. The useful discussions with R. T. Kado, E. Neher and U. Heinemann during initial stages of the work are gratefully acknowledged. I also thank Professors J. Dudel, R. Rüdel and Dr P. Honerjäger for reading the manuscript. The work was supported by the Deutsche Forschungsgemeinschaft, grant no. Ru 138/10 to Professor R. Rüdel.

REFERENCES

ALMERS, W. (1971). The potassium permeability of frog muscle membrane. *Ph.D. Thesis*, University of Rochester, Rochester, NY.

ARMSTRONG, C. M. (1975). K pores of nerve and muscle membranes. In *Membranes: a Series of Advances*, ed. EISENMAN, G. New York: Marcel Dekker.

ATTWELL, D. & COHEN, I. (1977). Voltage clamp of multicellular preparations. *Prog. Biophys. molec. Biol.* **31**, 201–245.

BAUMGARTEN, C. M. & ISENBERG, G. (1977). Depletion and accumulation of potassium in the extracellular clefts of cardiac Purkinje fibres during voltage clamp hyperpolarization and depolarization. *Pflügers Arch.* **368**, 19–31.

BEELER, G. W. & MCGUIGAN, J. A. S. (1978). Voltage clamping of multicellular myocardial preparations: capabilities and limitations of existing methods. *Prog. Biophys. molec. Biol.* **34**, 219–254.

BEELER, G. W. & REUTER, H. (1970). Voltage clamp experiments on ventricular myocardial fibres. *J. Physiol.* **207**, 165–190.

BEELER, G. W. & REUTER, H. (1977). Reconstruction of the action potential of ventricular myocardial fibres. *J. Physiol.* **268**, 177–210.

BOYETT, M. R., CORAY, A. & MCGUIGAN, J. A. S. (1980). Cow ventricular muscle. I. The effect of the extracellular potassium concentration on the current–voltage relationship. II. Evidence for a time dependent outward current. *Pflügers Arch.* **389**, 37–44.

CARMELIET, E. E. (1961). *Chloride and Potassium Permeability in Cardiac Purkinje Fibres*, Brussels: Editions Arsicia, S.A.

CARMELIET, E. E. & VERDONCK, F. (1977). Reduction of potassium permeability by chloride substitution in cardiac cells. *J. Physiol.* **265**, 193–206.

CHAPMAN, R. A. & FRY, C. H. (1978). An analysis of the cable properties of frog ventricular myocardium. *J. Physiol.* **283**, 263–383.

CLEEMANN, L. & MORAD, M. (1979*a*). Extracellular potassium accumulation in voltage-clamped frog ventricular muscle. *J. Physiol.* **286**, 83–111.

CLEEMANN, L. & MORAD, M. (1979*b*). Potassium currents in frog ventricular muscle: evidence from voltage clamp currents and extracellular K accumulation. *J. Physiol.* **286**, 113–143.

CLERC, L. (1976). Directional differences of impulse spread in trabecular muscle from mammalian heart. *J. Physiol.* **255**, 335–346.

CIANI, S., KRASNE, S., MIYAZAKI, S. & HAGIWARA, S. (1978). A model for anomalous rectification: electrochemical-potential-dependent gating of membrane channels. *J. Membrane Biol.* **44**, 103–134.

COHEN, I., DAUT, J. & NOBLE, D. (1976*a*). The effects of potassium and temperature on the pace-maker current, i_{K_2}, in Purkinje fibres. *J. Physiol.* **260**, 55–74.

COHEN, I., DAUT, J. & NOBLE, D. (1976*b*). An analysis of the actions of low concentrations of ouabain on membrane currents in Purkinje fibres. *J. Physiol.* **260**, 75–103.

COLATSKY, T. J. & TSIEN, R. W. (1979). Electrical properties associated with wide intercellular clefts in rabbit Purkinje fibres. *J. Physiol.* **290**, 227–252.

COLE, K. S. (1968). *Membranes, Ions and Impulses.* Berkeley and Los Angeles: University of California Press.

DAUT, J. & RÜDEL, R. (1979). A voltage clamp technique to measure the electrogenic pump current in mammalian myocardium. *Pflügers Arch.* **382**, R5.

DAUT, J. & RÜDEL, R. (1980). The electrogenic pump current in guinea-pig myocardium. *J. Physiol.* **305**, 22*P*.

DAUT, J. & RÜDEL, R. (1982). The electrogenic sodium pump in guinea-pig ventricular muscle: inhibition of pump current by cardiac glycosides. *J. Physiol.* **330**, 243–264.

DECK, K. A., KERN, R. & TRAUTWEIN, W. (1964). Voltage clamp technique in mammalian cardiac fibres. *Pflügers Arch.* **295**, 197–212.

DIFRANCESCO, D. & MCNAUGHTON, P. (1979). The effects of calcium on outward membrane currents in the cardiac Purkinje fibre. *J. Physiol.* **289**, 347–373.

DIFRANCESCO, D. & NOBLE, D. (1981). A model of cardiac electrical activity incorporating restricted extracellular spaces and the sodium–potassium pump. *J. Physiol.* **320**, 31*P*.

DREYER, F. & PEPER, K. (1974). Iontophoretic application of acetylcholine: advantages of high resistance micropipettes in connection with an electronic current pump. *Pflügers Arch.* **348**, 263–272.

DUDEL, J., PEPER, K., RÜDEL, R. & TRAUTWEIN, W. (1966). Excitatory membrane current in heart muscle (Purkinje fibres). *Pflügers Arch.* **292**, 255–273.

DUDEL, J., PEPER, K., RÜDEL, R. & TRAUTWEIN, W. (1967). The potassium component of membrane current in Purkinje fibres. *Pflügers Arch.* **296**, 308–327.

FOZZARD, H. A. & LEE, C. O. (1976). The influence of changes in external potassium and chloride ions on membrane potential and intracellular potassium ion activity in rabbit ventricular muscle. *J. Physiol.* **256**, 663–684.

GOERKE, J. & PAGE, E. (1965). Cat heart muscle *in vitro*. VI. Potassium exchange in papillary muscles. *J. gen. Physiol.* **48**, 933–948.

HAAS, H. G., GLITSCH, H. G. & KERN, R. (1977). Kalium-Fluxe und Membranpotential am Froschvorhof in Abhängigkeit von der Kalium-Aussenkonzentration. *Pflügers Arch.* **291**, 69–84.

HAGIWARA, S. & TAKAHASHI, K. (1974). The anomalous rectification and cation selectivity of the membrane of a starfish egg cell. *J. Membrane Biol.* **18**, 61–80.

HAGIWARA, S. & YOSHII, M. (1979). Effects of internal potassium and sodium on the anomalous rectification of the starfish egg as examined by internal perfusion. *J. Physiol.* **292**, 251–265.

HALL, A. E., HUTTER, O. F. & NOBLE, D. (1963). Current–voltage relations of Purkinje fibres in sodium-deficient solutions. *J. Physiol.* **166**, 225–240.

HILLE, B. & SCHWARZ, W. (1978). Potassium channels as multi-ion single-file pores. *J. gen. Physiol.* **72**, 409–442.

HODGKIN, A. L. & KATZ, B. (1949). The effect of sodium ions on the electrical activity on the giant axon of the squid. *J. Physiol.* **108**, 37–77.

HODGKIN, A. L. & RUSHTON, W. A. H. (1946). The electrical constants of a crustacean nerve fibre. *Proc. R. Soc.* B **133**, 444–479.

HORRES, C. R., AITON, J. F. & LIEBERMAN, M. (1979). Potassium permeability of embryonic avian heart cells in tissue culture. *Am. J. Physiol.* **236**, C163–C170.

HORRES, C. R. & LIEBERMAN, M. (1977). Compartmental analysis of potassium efflux from growth oriented heart cells. *J. Membrane Biol.* **34**, 331–350.

JACK, J. J. B., NOBLE, D. & TSIEN, R. W. (1975). *Electric Current Flow in Excitable Cells.* Oxford: Oxford University Press.

JOHNSON, E. A. & LIEBERMAN, M. (1971). Heart: excitation and contraction. *A. Rev. Physiol.* **33**, 479–532.

KAMIYAMA, A. & MATSUDA, K. (1966). Electrophysiological properties of the canine ventricular fibre. *Jap. J. Physiol.* **16**, 407–420.

KASS, R. S., SIEGELBAUM, S. A. & TSIEN, R. W. (1979). Three-micro-electrode voltage clamp experiments in calf cardiac Purkinje fibres: is slow inward current adequately measured? *J. Physiol.* **290**, 201–225.

KATZ, B. (1949). Les constantes électriques de la membrane du muscle. *Archs Sci. physiol.* **2**, 285–299.

LEECH, C. A. & STANFIELD, P. R. (1981). Dependence of inward rectification of frog skeletal muscle fibres on membrane potential and external potassium concentration. *J. Physiol.* **313**, 59*P*.

MCALLISTER, R. E., NOBLE, D. & TSIEN, R. W. (1975). Reconstruction of the electrical activity of cardiac Purkinje fibres. *J. Physiol.* **251**, 1–59.

MCDONALD, T. F. & TRAUTWEIN, W. (1978). The potassium current underlying delayed rectification in cat ventricular muscle. *J. Physiol.* **274**, 217–246.

MCGUIGAN, J. A. (1974). Some limitations of the double sucrose gap, and its use in a study of the slow inward current in mammalian ventricular muscle. *J. Physiol.* **240**, 775–806. With an Appendix by MCGUIGAN, J. A. S. & TSIEN, R. W.

MIROLLI, M. & TALBOTT, S. R. (1972). The geometrical factors determining the electronic properties of a molluscan neurone. *J. Physiol.* **227**, 19–34.

NEW, W. & TRAUTWEIN, W. (1972). Inward currents in mammalian myocardium. *Pflügers Arch.* **334**, 24–38.

NOBLE, D. (1965). Electrical properties of cardiac muscle attributable to inward going (anomalous) rectification. *J. cell. comp. Physiol.* **66**, Suppl., 127–135.

NOMA, A. & IRISAWA, H. (1976). Membrane currents in rabbit sinoatrial node cell as studied by the double microelectrode method. *Pflügers Arch.* **364**, 45–52.

OHMORI, H. (1978). Inactivation kinetics and steady-state noise in the anomalous rectifier of tunicate egg cell membrane. *J. Physiol.* **281**, 77–99.

PAGE, E. (1962). Cat heart muscle *in vitro* III. The extracellular space. *J. gen. Physiol.* **46**, 201–213.

PAGE, E. (1978). Quantitative ultrastructural analysis of cardiac membrane physiology. *Am. J. Physiol.* **235**, C147–158.

REUTER, H. (1979). Properties of two inward currents in the heart. *A. Rev. Physiol.* **41**, 413–424.

SAKAMOTO, Y. (1969). Membrane characteristics of the canine papillary muscle fibre. *J. gen. Physiol.* **54**, 765–781.

SAKAMOTO, Y. & GOTO, M. (1970). A study of the membrane constants in the dog myocardium. *Jap. J. Physiol.* **20**, 30–41.

SOMMER, J. R. & JOHNSON, E. A. (1968). Cardiac muscle: a comparative study of Purkinje fibres and ventricular fibres. *J. cell. Biol.* **36**, 497–526.

TANAKA, I. & SASAKI, Y. (1966). On the electrotonic spread in cardiac muscle of the mouse. *J. gen. Physiol.* **49**, 1089–1110.

TILLE, J. (1966). Electrotonic interaction between muscle fibres in the rabbit ventricle. *J. gen. Physiol.* **50**, 189–202.

TRAUTWEIN, W. (1973). Membrane currents in cardiac muscle fibres. *Physiol. Rev.* **53**, 793–835.

TRAUTWEIN, W. & MCDONALD, T. F. (1978). Current–voltage relations in ventricular muscle preparations from different species. *Pflügers Arch.* **374**, 79–89.

VAUGHAN-JONES, R. D. (1979*a*). Non-passive chloride distribution in mammalian heart muscle: micro-electrode measurement of the intracellular chloride activity. *J. Physiol.* **295**, 83–109.

VAUGHAN-JONES, R. D. (1979*b*). Regulation of chloride in quiescent sheep-heart Purkinje fibres studied using intracellular chloride and pH-sensitive micro-electrodes. *J. Physiol.* **295**, 111–137.

WEIDMANN, S. (1952). The electrical constants of Purkinje fibres. *J. Physiol.* **118**, 348–360.

WEIDMANN, S. (1966). The diffusion of radiopotassium across intercalated disks of mammalian cardiac muscle. *J. Physiol.* **187**, 323–342.

WEIDMANN, S. (1970). Electrical constants of trabecular muscle from mammalian heart. *J. Physiol.* **210**, 1041–1054.

WOODBURY, J. W. & CRILL, W. E. (1961). On the problem of impulses conduction in the atrium. In *Nervous Inhibition*. ed. FLOREY, E., pp. 124–135. Oxford: Pergamon Press.